



Aerobic alcohol oxidation catalyzed by supported ruthenium hydroxides

Kazuya Yamaguchi^{a,b}, Jung Won Kim^a, Jinling He^a, Noritaka Mizuno^{a,b,*}

^a Department of Applied Chemistry, School of Engineering, The University of Tokyo, 7-3-1 Hongo, Bunkyo-ku, Tokyo 113-8656, Japan

^b Core Research for Evolutional Science and Technology (CREST), Japan Science and Technology Agency (JST), 4-1-8 Honcho, Kawaguchi, Saitama 332-0012, Japan

ARTICLE INFO

Article history:

Received 2 September 2009

Revised 1 October 2009

Accepted 1 October 2009

Available online 31 October 2009

Keywords:

Alcohol oxidation

Heterogeneous catalysis

Molecular oxygen

Ruthenium hydroxide

ABSTRACT

The supported ruthenium hydroxide ($\text{Ru}(\text{OH})_x$) catalysts prepared with three different TiO_2 supports and an Al_2O_3 support showed the high catalytic activity for the oxidation of alcohols with molecular oxygen. In the presence of the most active catalyst, various kinds of alcohols could be converted into the corresponding carbonyl compounds in high yields. In addition, the catalyst could be applied to the aerobic amine oxidation. The observed catalysis was truly heterogeneous and the catalyst retrieved after the reaction could be reused with keeping its high catalytic performance. A reaction mechanism involving the ruthenium alcoholate formation/hydride abstraction (β -elimination) has been proposed. The alcoholate formation and hydride abstraction are reversible reactions. The kinetic isotope effects ($k_{\text{H}}/k_{\text{D}} = 4.9\text{--}5.3$) show that the C–H bond breaking is included in the rate-determining step. The present $\text{Ru}(\text{OH})_x$ -catalyzed aerobic alcohol oxidation was dependent on the coordination number (CN) of nearest-neighbor Ru atoms in $\text{Ru}(\text{OH})_x$ and the suitable CN existed.

© 2009 Elsevier Inc. All rights reserved.

1. Introduction

The oxidation of alcohols is of paramount importance in organic syntheses in laboratories as well as chemical industries because of the versatile use of products such as aldehydes and ketones as important intermediates for pharmaceuticals, agricultural chemicals, and fine chemicals [1–5]. Until now, many efficient heterogeneous catalysts based on noble metal clusters, metal oxides, and metal hydroxides have been developed for the oxidation of alcohols with molecular oxygen as a sole oxidant [6,7]. The scope and limitation of heterogeneously catalyzed aerobic alcohol oxidation systems have been summarized in the recent excellent review articles [6,7]. Among heterogeneous catalysts, we [8,9] and other research groups [10–13] focused on ruthenium hydroxide $\text{Ru}(\text{OH})_x$ (hydrate oxide $\text{RuO}_2 \cdot x\text{H}_2\text{O}$) for the aerobic alcohol oxidation.

Matsumoto and Watanabe first reported that $\text{Ru}(\text{OH})_x$ ($\text{RuO}_2 \cdot x\text{H}_2\text{O}$) could catalyze the aerobic oxidation of allylic alcohols [10]. The turnover number (TON) and turnover frequency (TOF) were low and the applicability was limited to only allylic alcohols [10]. In 2002, we reported that $\text{Ru}(\text{OH})_x$ supported on Al_2O_3 ($\text{Ru}(\text{OH})_x/\text{Al}_2\text{O}_3$) could act as an efficient reusable heterogeneous catalyst for the aerobic oxidation of various kinds of structurally diverse alcohols including benzylic, allylic, aliphatic, and heteroatom-containing ones [8]. Besides the aerobic alcohol oxidation, many

functional group transformations such as the oxidative dehydrogenation and oxygenation of amines [14,15], hydration of nitriles [16], and hydrogen-transfer reactions [17,18] also efficiently proceeded with $\text{Ru}(\text{OH})_x/\text{Al}_2\text{O}_3$. The outstanding catalytic performance is likely attributed to the presence of coordinatively unsaturated ruthenium centers (Lewis acid sites) [19–21] and basic hydroxide groups (Brønsted base sites) [21]. After our first report for the supported $\text{Ru}(\text{OH})_x$ catalyst [8], $\text{Ru}(\text{OH})_x$ supported on zeolites [11], titanium oxide nanotubes [12], and carbon nanotubes [13] have been reported to be active for the aerobic alcohol oxidation.

It has been reported that $\text{Ru}(\text{OH})_x$ has one-dimensional chain-like core structure [11,21,22]. It is very difficult to control the structure and size of (unsupported) $\text{Ru}(\text{OH})_x$ because the dehydrative condensation easily proceeds upon the heat treatment (>ca. 100 °C) [22]. Very recently, we have successfully prepared highly dispersed $\text{Ru}(\text{OH})_x$ on metal oxide supports such as TiO_2 and Al_2O_3 [21]. The coordination numbers (CNs) of one-dimensional chain-like $\text{Ru}(\text{OH})_x$ could be controlled by choosing appropriate supports and the supported $\text{Ru}(\text{OH})_x$ catalysts were highly thermally stable under reaction conditions (up to ca. 150 °C) [21]. This offered an opportunity to investigate the CN-dependent catalytic activity of the $\text{Ru}(\text{OH})_x$ species. For example, the reaction rates (TOFs) for the hydrogen-transfer reactions such as the racemization of chiral secondary alcohols and Meerwein–Ponndorf–Verley-type (MPV-type) reduction of carbonyl compounds were much dependent on the CNs of $\text{Ru}(\text{OH})_x$ and monotonically increased with the decrease in the CNs (Fig. S1) [21]. As for the aerobic alcohol oxidation, no studies have been devoted to address the

* Corresponding author. Address: Department of Applied Chemistry, School of Engineering, The University of Tokyo, 7-3-1 Hongo, Bunkyo-ku, Tokyo 113-8656, Japan. Fax: +81 3 5841 7220.

E-mail address: tmizuno@mail.ecc.u-tokyo.ac.jp (N. Mizuno).

relationship between the CNs of Ru(OH)_x and the catalytic activity, as far as we know. In this study, the supported Ru(OH)_x catalysts with the different CNs were utilized for the aerobic alcohol oxidation and the CN-dependent catalytic activity was examined. In addition, the scope of the present Ru(OH)_x-catalyzed aerobic alcohol oxidation and possible reaction mechanism were also investigated in detail.

2. Experimental section

2.1. General

The NMR spectra were recorded on JEOL JNM-EX-270. The ¹H and ¹³C NMR spectra were measured at 270 and 67.8 MHz, respectively, in [D₁]chloroform or [D₈]toluene with TMS as an internal standard. The GC analyses were performed on Shimadzu GC-17A using a flame ionization detector (FID) equipped with a DB-WAX capillary column (internal diameter = 0.25 mm, length = 30 m) or a Rt β-CDEXM capillary column (internal diameter = 0.25 mm, length = 30 m). The mass spectra were recorded on Shimadzu GCMS-QP2010 equipped with a TC-5HT capillary column (internal diameter = 0.25 mm, length = 30 m). The ICP-AES analyses were performed with Shimadzu ICPS-8100. The X-ray absorption spectra were recorded at the NW10A beamline of PF at KEK, Japan (proposal No. 2007G096) [21]. The data were analyzed using REX2000 software (version 2.5, Rigaku) [21]. The heterolytic benzylic C–H bond dissociation energies of *p*-substituted benzyl alcohols were calculated at the B3LYP/6-311++G(d, p) level theory with Gaussian 03 program package [23].

2.2. Reagents and catalysts

Substrates and solvents were commercially obtained from Tokyo Kasei, Aldrich, and Fluka (reagent grade) and purified before the use [24]. Anatase TiO₂ (TiO₂(A), BET surface area: ST-01, 316 m² g⁻¹), anatase TiO₂ (TiO₂(B), JRC-TIO-1, 73 m² g⁻¹), rutile TiO₂ (TiO₂(C), SUPER-TITANIA G-2, 3.2 m² g⁻¹), and Al₂O₃ (KHS-24, 160 m² g⁻¹) were obtained from Ishihara Sangyo Kaisya Ltd., the Catalysis Society of Japan, Showa Denko K.K., and Sumitomo Chemical, respectively. RuHAP (9.1 wt%) was purchased from Wako. The supported Ru(OH)_x catalysts and Ru(OH)_x were prepared according to the literature procedures (see Supporting information) [21].

2.3. Catalytic aerobic oxidation

A suspension of the supported Ru(OH)_x catalyst in a solvent was stirred for 5 min. Then, a substrate was added and molecular oxygen was passed through the suspension. The mixture was stirred (800 rpm) at reaction temperature under 1 atm of molecular oxygen. The yield and product selectivity were periodically deter-

mined by GC analysis. All products have been identified by comparison of their ¹H and ¹³C NMR, and mass spectra with the literature data. The retrieved catalyst was washed with an aqueous solution of NaOH (pH 13) and water, and then dried in vacuo before being recycled. The TOF values were calculated based on the total Ru in the catalysts.

3. Results and discussion

3.1. The effect of catalysts on the aerobic alcohol oxidation

We prepared four kinds of supported Ru(OH)_x catalysts (Ru(OH)_x/support) with three different TiO₂ supports (anatase TiO₂ (TiO₂(A), BET surface area: 316 m² g⁻¹), anatase TiO₂ (TiO₂(B), 73 m² g⁻¹), and rutile TiO₂ (TiO₂(C), 3.2 m² g⁻¹)) and an Al₂O₃ support (160 m² g⁻¹) (Table 1, see Supporting information for preparation). The ruthenium contents in Ru(OH)_x/TiO₂(A), Ru(OH)_x/TiO₂(B), Ru(OH)_x/TiO₂(C), and Ru(OH)_x/Al₂O₃ were 2.1, 2.2, 2.2, and 2.1 wt%, respectively (Table 1). The detailed structural characterization of these catalysts has been reported elsewhere [21]. The CNs of the nearest-neighbor Ru atoms (EXAFS analysis, Table 1, Table S1 and Fig. S2) decreased in the order of Ru(OH)_x/TiO₂(C) > Ru(OH)_x/Al₂O₃ > Ru(OH)_x/TiO₂(B) > Ru(OH)_x/TiO₂(A) [21].

First, the catalytic activities for the oxidation of 1-phenylethanol (**1a**) to acetophenone (**2a**) with 1 atm of molecular oxygen were compared among various ruthenium catalysts (Table 2). The supported Ru(OH)_x catalysts showed high catalytic performance for the oxidation (Table 2, entries 1–4). Among the supported Ru(OH)_x catalysts examined, the observed TOFs (TOF_{obs}) increased in the order of Ru(OH)_x/TiO₂(C) (TOF_{obs} = 75 h⁻¹) < Ru(OH)_x/Al₂O₃ (90 h⁻¹) < Ru(OH)_x/TiO₂(A) (100 h⁻¹) < Ru(OH)_x/TiO₂(B) (160 h⁻¹) (see the later section), while the selectivities to **2a** were >99% in all cases. The TOF_{obs} value of the most active Ru(OH)_x/TiO₂(B) catalyst was about twice higher than that of the previously reported Ru(OH)_x/Al₂O₃ [8,9].

No reaction proceeded in the absence of the catalysts or in the presence of supports such as TiO₂ and Al₂O₃ (Table 2, entries 14–18). The oxidation hardly proceeded in the presence of Ru(OH)_x and anhydrous RuO₂ (Table 2, entries 5 and 6). The catalytic activity of RuHAP (Ru–Cl species supported on hydroxyapatite) [25] was much lower than those of the supported Ru(OH)_x catalysts (Table 2, entry 7). In the case of the catalyst precursor of RuCl₃·*n*H₂O, the selectivity to **2a** was very low because of the formation of 1-phenyl-1-tolylethane and 1,1'-(oxydiethylidene)-bis-benzene as byproducts (Table 2, entry 8). Although RuCl₂(PPh₃)₃ was reported to be active for the aerobic alcohol oxidation in the presence of 2,2',6,6'-tetramethylpiperidine *N*-oxyl (TEMPO) [26] and hydroquinone [27], it gave only a stoichiometric amount of **2a** in the absence of these additives (Table 2, entry 9). Other ruthenium complexes such as RuCl₂(bpy)₂, [RuCl₂(benzene)]₂, Ru(acac)₃, and Ru₃(CO)₁₂ were completely inactive (Table 2, entries 10–13).

Table 1
Various supported Ru(OH)_x catalysts.

Catalyst (wt%)	Support ^a	BET surface area (m ² g ⁻¹)		CN ^b	<i>d</i> (Å) ^c
		Support	Catalyst		
Ru(OH) _x /TiO ₂ (A) (2.1)	Anatase TiO ₂	316	298	0.37 (±0.17)	3.07 (±0.02)
Ru(OH) _x /TiO ₂ (B) (2.2)	Anatase TiO ₂	73	74	0.76 (±0.21)	3.09 (±0.01)
Ru(OH) _x /TiO ₂ (C) (2.2)	Rutile TiO ₂	3.2	7.0	0.94 (±0.22)	3.10 (±0.01)
Ru(OH) _x /Al ₂ O ₃ (2.1)	Al ₂ O ₃	160	163	0.91 (±0.20)	3.08 (±0.01)
Ru(OH) _x	–	–	15	1.4 (±0.2)	3.10 (±0.01)

^a See Section 2.

^b CN = average coordination number of nearest-neighbor Ru atoms.

^c *d* = average interatomic Ru···Ru distance.

Table 2The aerobic oxidation of **1a** by various catalysts.^a

Entry	Catalyst	Conversion of 1a (%)	Selectivity to 2a (%)	TOF _{obs} (h ⁻¹) ^b
1	Ru(OH) _x /TiO ₂ (A)	49	>99	100
2	Ru(OH) _x /TiO ₂ (B)	62	>99	160
3	Ru(OH) _x /TiO ₂ (C)	27	>99	75
4	Ru(OH) _x /Al ₂ O ₃	45	>99	90
5	Ru(OH) _x	No reaction	–	–
6	RuO ₂ (anhydrous)	No reaction	–	–
7	RuHAP	2	>99	1.0
8	RuCl ₃ · <i>n</i> H ₂ O	>99	<1 ^c	–
9	RuCl ₂ (PPh ₃) ₃	1	>99	0.5
10	RuCl ₂ (bpy) ₂	No reaction	–	–
11	[RuCl ₂ (benzene)] ₂	No reaction	–	–
12	Ru(acac) ₃	No reaction	–	–
13	Ru ₃ (CO) ₁₂	No reaction	–	–
14 ^d	TiO ₂ (A)	No reaction	–	–
15 ^d	TiO ₂ (B)	No reaction	–	–
16 ^d	TiO ₂ (C)	No reaction	–	–
17 ^d	Al ₂ O ₃	No reaction	–	–
18	None	No reaction	–	–

^a Reaction conditions: **1a** (1 mmol), catalyst (Ru: 1 mol%), toluene (3 mL), 80 °C, 0.5 h, under 1 atm of molecular oxygen. Conversion and selectivity were determined by GC using an internal standard.

^b Based on the observed reaction rate.

^c 1-Phenyl-1-tolyethane and 1,1'-(oxydiethylidene)-bis-benzene were formed as byproducts.

^d 40 mg.

3.2. The scope of the present aerobic oxidation

In the presence of the most active Ru(OH)_x/TiO₂(B) catalyst, the aerobic oxidation of various kinds of structurally diverse alcohols was examined (Table 3). Secondary (**1a–1d**) and primary (**1e–1h**) benzylic alcohols were oxidized to afford the corresponding carbonyl compounds in quantitative yields (Table 3, entries 1–8). Notably, the oxidation efficiently proceeded even at room temperature (ca. 25 °C) (Scheme 1). The oxidation of **1c** with the unstable cyclopropane ring exclusively proceeded to give the corresponding ketone **2c** without formation of the ring-opened products (Table 3, entry 3). It has been reported that **1d** gave the corresponding ketone **2d** with two-electron transfer oxidants and that **2e** and *tert*-butyl radical were obtained as primary products with one-electron transfer oxidants (radical mechanism) [28]. In the present Ru(OH)_x/TiO₂(B)-catalyzed system, the corresponding ketone **2d** was exclusively obtained as a sole product without the formation of **2e** (Table 3, entry 4). In the case of **1i**, the corresponding unsaturated aldehyde **2i** was obtained without the intramolecular hydrogen-transfer reaction and geometrical isomerization of the carbon–carbon double bond (Table 3, entry 9). The present system could oxidize linear (**1j**) and cyclic aliphatic (**1k**) alcohols in high yields (Table 3, entries 10 and 11). Also, Ru(OH)_x/TiO₂(B) efficiently catalyzed the oxidation of heteroatom-containing alcohols such as **1l** and **1m** (Table 3, entries 12 and 13). In addition, the present system could be applied to the aerobic oxidation of secondary (**3a** and **3b**) and primary (**3c**)¹ amines (Table 3, entries 14–16).

In order to verify whether the observed catalysis is derived from solid Ru(OH)_x/TiO₂(B) or leached ruthenium species, the oxidation of **1a** was carried out under the conditions described in Table 3 and

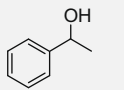
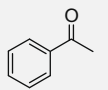
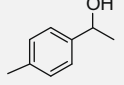
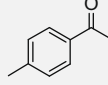
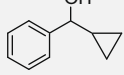
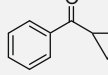
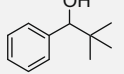
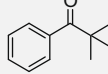
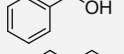
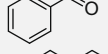
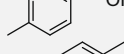
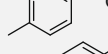
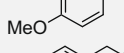
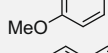
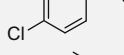
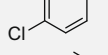
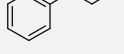
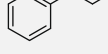
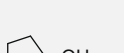
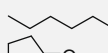
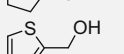
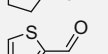
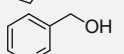
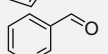
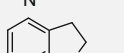
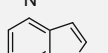
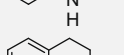
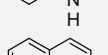
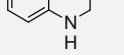
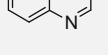
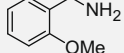
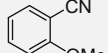
the Ru(OH)_x/TiO₂(B) catalyst was removed from the reaction mixture by hot filtration at ca. 50% conversion of **1a**. After removal of the catalyst, the reaction was again carried out with the filtrate under the same conditions. In this case, the reaction was completely stopped. It was confirmed by the ICP-AES analysis that no ruthenium was detected in the filtrate (below detection limit of 7 ppb). All these facts can rule out any contribution to the observed catalysis from ruthenium species that leached into the reaction solution and the observed catalysis is intrinsically heterogeneous [29]. In addition, it was confirmed by XANES and EXAFS spectra that the local structure of the ruthenium species in the used Ru(OH)_x/TiO₂(B) catalyst was the same as that in the fresh catalyst (Fig. S3). The Ru(OH)_x/TiO₂(B) catalyst could be reused for the oxidation of **1a** at least three times with retention of its high catalytic performance (>99% yield of **2a** for the third reuse experiment).

3.3. Mechanistic studies

The reaction mechanism for the present aerobic oxidation of alcohols was examined with the most active Ru(OH)_x/TiO₂(B) catalyst. The addition of a radical scavenger of 2,6-di-*tert*-butyl-4-methylphenol (1 mol% with respect to **1a**) did not affect the reaction rate and product selectivity for the oxidation of **1a**. Furthermore, the oxidations of **1c** and **1d** exclusively proceeded to give the corresponding ketones **2c** and **2d** without the formation of ring-opened and cleaved products, respectively (Table 3, entries 3 and 4). These results show that free-radical intermediates are not involved in the present alcohol oxidation. In the competitive oxidation of **1a** and **1e**, the oxidation of a primary alcohol **1e** proceeded much faster than that of a secondary alcohol **1a** (Fig. 1). The faster oxidation of a primary alcohol in the presence of a secondary one suggests the formation of an alcoholate species via the ligand exchange between the ruthenium hydroxide species and an alcohol [25–27,30–33].

¹ For the oxidation of primary amines with Ru(OH)_x/TiO₂(B), the selectivities to the desired nitriles were lower (by ca. 10%) than those with Ru(OH)_x/Al₂O₃. This is likely due to the decomposition of the intermediate imines by the acidic TiO₂ support.

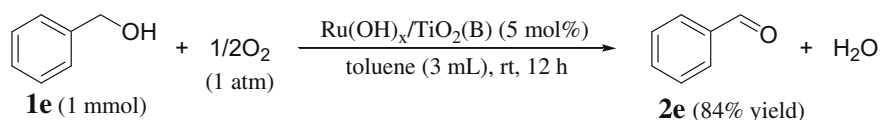
Table 3
The aerobic oxidation of various alcohols and amines catalyzed by Ru(OH)_x/TiO₂(B).^a

Entry	Substrate		Time (min)	Conversion (%)	Product		Selectivity (%)
1		1a	120	>99		2a	>99
2		1b	72	>99		2b	>99
3		1c	60	>99		2c	>99
4		1d	60	>99		2d	>99
5		1e	60	>99		2e	>99
6		1f	40	>99		2f	>99
7		1g	40	>99		2g	>99
8		1h	60	>99		2h	>99
9		1i	420	>99		2i	>99
10 ^b		1j	180	84		2j	>99
11		1k	180	76		2k	>99
12 ^c		1l	360	>99		2l	>99
13 ^c		1m	270	>99		2m	>99
14		3a	150	99		4a	>99
15		3b	210	74		4b	>99
16		3c	240	>99		4c	76

^a Typical reaction conditions: substrate (1 mmol), Ru(OH)_x/TiO₂(B) (Ru: 1 mol% for alcohols, 3 mol% for amines), toluene (3 mL), 80 °C for alcohols, 100 °C for amines, under 1 atm of molecular oxygen. Yields were determined by GC analyses using an internal standard.

^b 2 mol%.

^c 5 mol%.



Scheme 1. The Ru(OH)_x/TiO₂(B)-catalyzed oxidation of **1e** at room temperature.

The Ru(OH)_x/TiO₂(B)-catalyzed competitive oxidations of *p*-substituted benzyl alcohols gave the following reactivity order: *p*-CH₃O (*R_x*/*R_H* = 2.4) > *p*-CH₃ (1.6) > *p*-H (1.0) > *p*-Cl (0.95) (the values in the parentheses were the relative rates and the rate of **1e** (*p*-H) was taken as a unity). The relative rates (log(*R_x*/*R_H*)) are plotted against the heterolytic benzylic C–H bond dissociation energies of *p*-substituted benzyl alcohols calculated at the B3LYP/6-311++G(d, p) level theory (Fig. 2). The good linear correlation was ob-

served, suggesting the formation of the carbocation-type transition state *via* the hydride abstraction. The formation of the ruthenium hydride species was evidenced by the fact that Ru(OH)_x/TiO₂(B) showed high catalytic activity for the hydrogen-transfer reactions such as the racemization of chiral secondary alcohols and MPV-type reduction of carbonyl compounds using 2-propanol [21].

On the basis of the above results, we here propose a possible reaction mechanism as shown in Scheme 2. The mechanism is

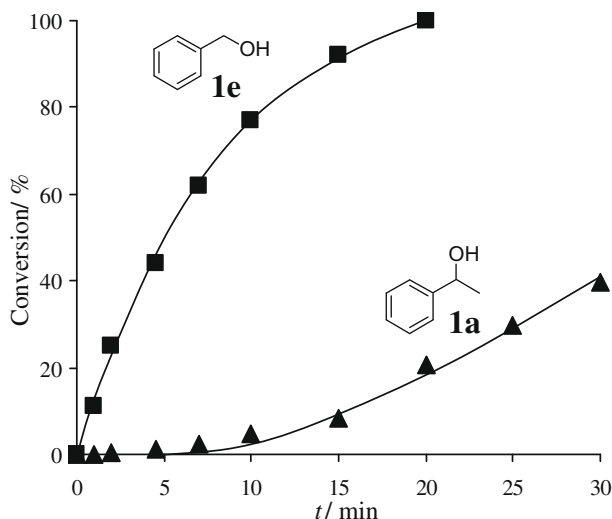


Fig. 1. The reaction profiles of the competitive oxidation of **1a** and **1e**. Reaction conditions: **1a** (0.5 mmol), **1e** (0.5 mmol), Ru(OH)_x/TiO₂(B) (Ru: 1 mol%), toluene (3 mL), 80 °C, under 1 atm of molecular oxygen.

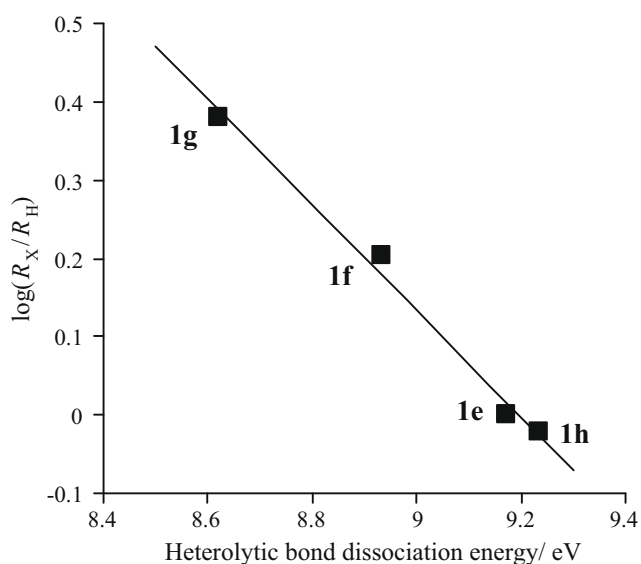
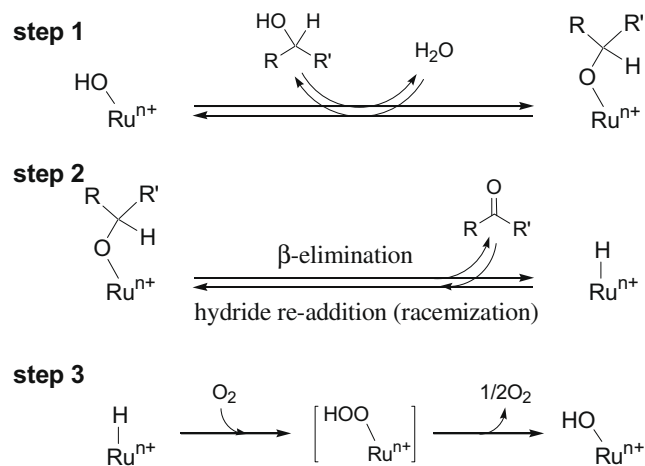


Fig. 2. The relationship between the relative rates ($\log(R_x/R_H)$) and heterolytic benzylic C–H bond dissociation energies of *p*-substituted benzyl alcohols. Reaction conditions: **1e** (0.5 mmol), *p*-substituted benzyl alcohol (**1f**, **1g**, or **1h**, 0.5 mmol), Ru(OH)_x/TiO₂(B) (Ru: 1 mol%), toluene (3 mL), 80 °C, under 1 atm of molecular oxygen.

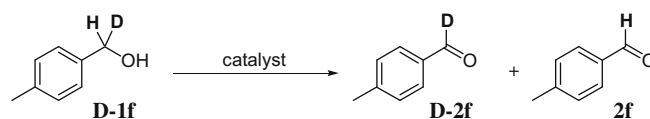
intrinsically the same as the widely accepted one with Ru(OH)_x-based catalysts [8–13]. First, the ruthenium alcoholate species is formed (step 1). No kinetic isotope effect was observed for the oxidation of 2-propanol-OD. Thus, the ligand exchange between the ruthenium hydroxide and an alcohol is very fast and is not the rate-determining step. Then, the typical β-elimination proceeds to give the corresponding carbonyl compound and the ruthenium hydride species (step 2). This step is reversible because the oxidation of a chiral secondary alcohol proceeds with a simultaneous decrease in the enantiomeric excess (*ee*) of the substrate (see the later section). Finally, the hydride species is reoxidized by molecular oxygen (step 3). The amine oxidation proceeds in a similar way; the formation of ruthenium amide species followed by the β-elimination [14]. The reaction rates for the oxidation of **1a** were almost independent of the partial pressure of molecular oxygen (>0.5 atm,



Scheme 2. A proposed reaction mechanism for the present Ru(OH)_x-catalyzed aerobic oxidation of alcohols.

Table 4

The kinetic isotope effects for the oxidation of **D-1f**^a.



Entry	Catalyst	Yield (%)		<i>k_H</i> / <i>k_D</i>
		D-2f	2f	
1	Ru(OH) _x /TiO ₂ (A)	83	17	4.9
2	Ru(OH) _x /TiO ₂ (B)	84	16	5.3
3	Ru(OH) _x /Al ₂ O ₃	75	15	5.0
4	Ru(OH) _x /TiO ₂ (C)	60	12	5.1
5	Ru(OH) _x	No reaction		

^a Reaction conditions: **D-1f** (0.5 mmol), catalyst (Ru: 1 mol%), [D₈]toluene (1.5 mL), 80 °C, 1.5 h, under 1 atm of molecular oxygen. Yields were determined by ¹H NMR.

Fig. S4). The *k_H*/*k_D* values (kinetic isotope effects) for the oxidation of α-deuterio-*p*-methylbenzyl alcohol (**D-1f**) with the supported Ru(OH)_x catalysts were in the range of 4.9–5.3 (Table 4). These results show that the C–H bond breaking (step 2) is included in the rate-determining step in all cases with supported Ru(OH)_x catalysts [34].

3.4. The reason why the CN-dependent catalytic activity is observed for the aerobic alcohol oxidation

As mentioned in the previous section (Table 2), the TOF_{Sobs} for the oxidation of **1a** increased in the order of Ru(OH)_x/TiO₂(C) (TOF_{Sobs} = 75 h⁻¹) < Ru(OH)_x/Al₂O₃ (90 h⁻¹) < Ru(OH)_x/TiO₂(A) (100 h⁻¹) < Ru(OH)_x/TiO₂(B) (160 h⁻¹). The TOF_{Sobs} are plotted against the CNs of nearest-neighbor Ru atoms in the supported Ru(OH)_x catalysts (Fig. 3). The TOF_{Sobs} increased with the decrease in the CNs, reached maximum with Ru(OH)_x/TiO₂(B), and then decreased.²

² For the aerobic oxidation of **3a**, the TOF_{Sobs} also increased with the decrease in the CNs, reached maximum with Ru(OH)_x/TiO₂(B), and then decreased (Fig. S5).

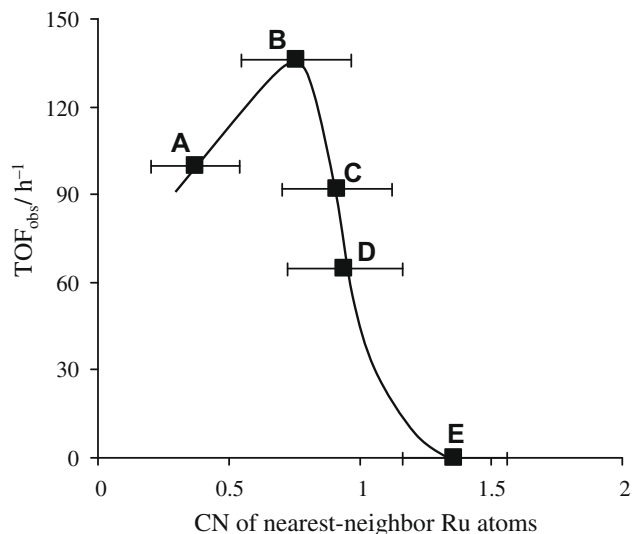


Fig. 3. The relationship between TOF_{obs} and CNs of nearest-neighbor Ru atoms for the aerobic oxidation of **1a**. (A) $\text{Ru}(\text{OH})_x/\text{TiO}_2(\text{A})$, (B) $\text{Ru}(\text{OH})_x/\text{TiO}_2(\text{B})$, (C) $\text{Ru}(\text{OH})_x/\text{Al}_2\text{O}_3$, (D) $\text{Ru}(\text{OH})_x/\text{TiO}_2(\text{C})$, and (E) $\text{Ru}(\text{OH})_x$. Reaction conditions: **1a** (1 mmol), catalyst (Ru: 1 mol%), toluene (3 mL), 80 °C, under 1 atm of O_2 .

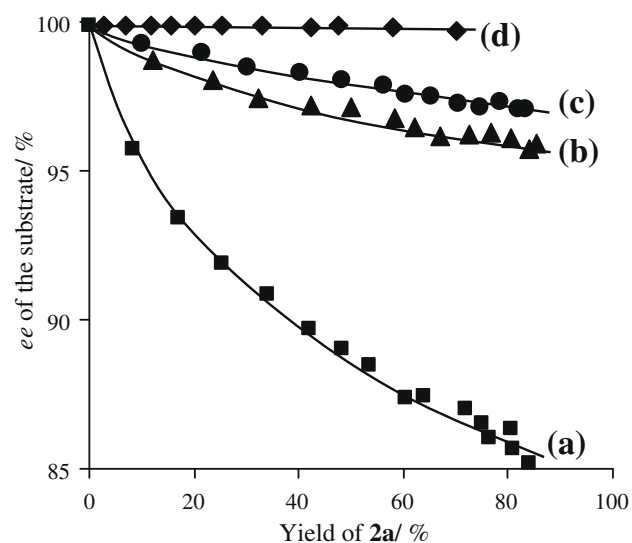


Fig. 4. The *ee* of the substrate vs. yield of **2a** plots for the oxidation of **1a** with (a) $\text{Ru}(\text{OH})_x/\text{TiO}_2(\text{A})$ and (b) $\text{Ru}(\text{OH})_x/\text{TiO}_2(\text{B})$, (c) $\text{Ru}(\text{OH})_x/\text{Al}_2\text{O}_3$, and (d) $\text{Ru}(\text{OH})_x/\text{TiO}_2(\text{C})$. Reaction conditions: **1a** (1 mmol), catalyst (Ru: 1 mol%), toluene (3 mL), 80 °C, under 1 atm of O_2 .

Next, the aerobic oxidations of (*R*)-1-phenylethanol (**1a**, >99% *ee*) were carried out with a series of the supported $\text{Ru}(\text{OH})_x$ catalysts, and the yields of **2a** and *ees* of the substrate were monitored during the oxidation. As shown in Fig. 4, the oxidation of **1a** proceeded with a simultaneous decrease in the *ees* in all cases, showing that the progress of the racemization of **1a** by the re-addition of the hydride species (backward reaction in step 2) even under aerobic conditions. The TOFs for the racemization based on the initial rates (TOF_{rac})³ monotonically increased with the decrease in the CNs of nearest-neighbor Ru atoms and the order was as follows: $\text{Ru}(\text{OH})_x/\text{TiO}_2(\text{C})$ ($\text{TOF}_{\text{rac}} = 0.20 \text{ h}^{-1}$) < $\text{Ru}(\text{OH})_x/\text{Al}_2\text{O}_3$

Table 5
The TOF_{obs} , TOF_{rac} , and $\text{TOF}_{\beta\text{-elim}}$ values for the oxidation of **1a**.^a

Entry	Catalyst	TOF_{obs} (h^{-1}) ^b	TOF_{rac} (h^{-1}) ^c	$\text{TOF}_{\beta\text{-elim}}$ (h^{-1}) ^d
1	$\text{Ru}(\text{OH})_x/\text{TiO}_2(\text{A})$	100	52	152
2	$\text{Ru}(\text{OH})_x/\text{TiO}_2(\text{B})$	136	10	146
3	$\text{Ru}(\text{OH})_x/\text{Al}_2\text{O}_3$	92	2.6	95
4	$\text{Ru}(\text{OH})_x/\text{TiO}_2(\text{C})$	65	0.20	65
5	$\text{Ru}(\text{OH})_x$	No reaction		

^a Reaction conditions: **1a** (1 mmol), catalyst (Ru: 1 mol%), toluene (3 mL), 80 °C, under 1 atm of molecular oxygen.

^b Based on the observed reaction rate.

^c Based on the initial rate. $\text{TOF}_{\text{rac}} (\text{h}^{-1}) = \{\log(ee/100)\} / \{\log(1 - (x/100))\} / t$, where *ee*, *x*, and *t* are the enantiomeric excess (%), total amount of Ru in the catalyst (mol%), and reaction time (h), respectively.

^d $\text{TOF}_{\beta\text{-elim}} (\text{h}^{-1}) = \text{TOF}_{\text{obs}} (\text{h}^{-1}) + \text{TOF}_{\text{rac}} (\text{h}^{-1})$.

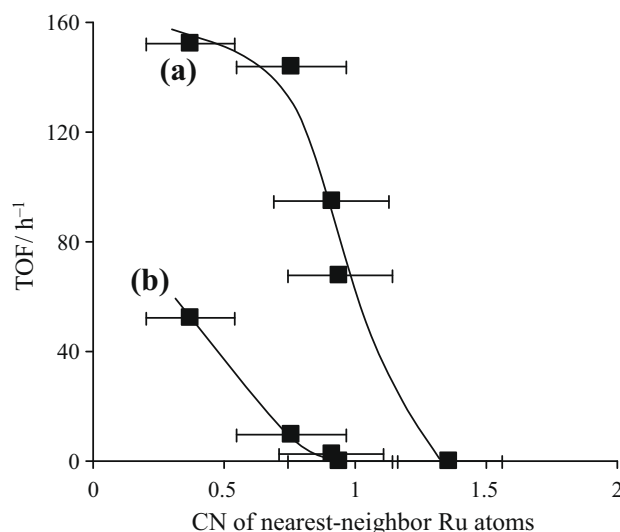


Fig. 5. The relationship between TOFs ((a) $\text{TOF}_{\beta\text{-elim}}$ and (b) TOF_{rac}) and CNs of nearest-neighbor Ru atoms for the aerobic oxidation of **1a**. Reaction conditions: **1a** (1 mmol), catalyst (Ru: 1 mol%), toluene (3 mL), 80 °C, under 1 atm of O_2 .

(2.6 h^{-1}) < $\text{Ru}(\text{OH})_x/\text{TiO}_2(\text{B})$ (10 h^{-1}) < $\text{Ru}(\text{OH})_x/\text{TiO}_2(\text{A})$ (52 h^{-1}) (Table 5 and Fig. 5b). This order was well consistent with that for the racemization under anaerobic conditions (Fig. S1) [21].

As mentioned in the previous section: (i) no kinetic isotope effect was observed for 2-propanol-OD, (ii) the kinetic isotope effects for the oxidation of **D-1f** with the supported $\text{Ru}(\text{OH})_x$ catalysts were in the range of 4.9–5.3 (Table 4), and (iii) the reaction rates were almost independent of the partial pressure of molecular oxygen (Fig. S4), showing that the step 2 is the rate-determining step for the present oxidation. Therefore, the TOF_{obs} corresponds to that for the step 2, i.e., $\text{TOF}_{\beta\text{-elim}} - \text{TOF}_{\text{rac}}$, where $\text{TOF}_{\beta\text{-elim}}$ is the TOF for the β -elimination (forward reaction in step 2). The $\text{TOF}_{\beta\text{-elim}}$ with $\text{Ru}(\text{OH})_x/\text{TiO}_2(\text{A})$, $\text{Ru}(\text{OH})_x/\text{TiO}_2(\text{B})$, $\text{Ru}(\text{OH})_x/\text{Al}_2\text{O}_3$, and $\text{Ru}(\text{OH})_x/\text{TiO}_2(\text{C})$ were calculated to be 152, 146, 95, and 65 h^{-1} , respectively (Table 5 and Fig. 5a). The $\text{TOF}_{\beta\text{-elim}}$ and TOF_{rac} (for forward and backward reactions in step 2) intrinsically increased with the decrease in the CNs of nearest-neighbor Ru atoms (Fig. 5), likely because of the increase in the numbers of coordinatively unsaturated sites [19–21]. The TOF_{rac} more increased than $\text{TOF}_{\beta\text{-elim}}$ with the decrease in CNs from 0.76 to 0.37 (Fig. 5b), while the $\text{TOF}_{\beta\text{-elim}}$ more increased than TOF_{rac} with the decrease in CNs from 0.94 to 0.76 (Fig. 5a). Therefore, the $\text{Ru}(\text{OH})_x/\text{TiO}_2(\text{B})$ catalyst with the suitable CNs showed the highest catalytic activity for the present aerobic alcohol oxidation (Fig. 3).

³ The TOF_{rac} based on the initial rates can be calculated by the following recursion formula [17]: $\text{TOF}_{\text{rac}} (\text{h}^{-1}) = \{\log(ee/100)\} / \{\log(1 - (x/100))\} / t$, where *ee*, *x*, and *t* are the enantiomeric excess (%), total amount of Ru in the catalyst (mol%), and reaction time (h), respectively.

4. Conclusions

The Ru(OH)_x-catalyzed aerobic alcohol oxidation was structure-dependent. The catalytic activities of Ru(OH)_x for both the β-elimination (hydride abstraction) and racemization (hydride re-addition) intrinsically increased with the decrease in the CNs of nearest-neighbor Ru atoms (the size of Ru(OH)_x species). The TOFs for the racemization more increased than those of β-elimination with the decrease in CNs from 0.76 to 0.37, while the TOFs for the β-elimination more increased than those of racemization with the decrease in CNs from 0.94 to 0.76. As a result, the observed TOFs increased with the decrease in the CNs, reached maximum with Ru(OH)_x/TiO₂(B), and then decreased. In the presence of the most active Ru(OH)_x/TiO₂(B), various kinds of structurally diverse alcohols including benzylic, allylic, aliphatic, and heteroatom-containing ones could be converted into the corresponding carbonyl compounds in high to excellent yields. Moreover, the catalyst could be applied to the aerobic amine oxidation. The observed catalysis was truly heterogeneous in nature and the Ru(OH)_x/TiO₂(B) catalyst retrieved after the reaction could be reused without an appreciable loss of its high catalytic activity for the aerobic oxidation.

Acknowledgments

We thank Mr. T. Koike (The University of Tokyo) for his help with experiments. This work was supported in part by the Core Research for Evolutional Science and Technology (CREST) program of the Japan Science and Technology Agency (JST), the Global COE Program (Chemistry Innovation through Cooperation of Science and Engineering), and Grants-in-Aid for Scientific Researches from Ministry of Education, Culture, Sports, Science and Technology.

Appendix A. Supplementary material

Supplementary data associated with this article can be found, in the online version, at [doi:10.1016/j.jcat.2009.10.004](https://doi.org/10.1016/j.jcat.2009.10.004).

References

- [1] R.A. Sheldon, J.K. Kochi, *Metal Catalyzed Oxidations of Organic Compounds*, Academic Press, New York, 1981. p. 1.
- [2] M. Hudlicky, *Oxidations in Organic Chemistry*, ACS Monograph Series, American Chemical Society, Washington, DC, 1990. p. 1.
- [3] S.V. Ley, J. Norman, W.P. Griffith, S.P. Marsden, *Synthesis* (1994) 639.
- [4] R.A. Sheldon, I.W.C.E. Arends, D. Dijksman, *Catal. Today* 57 (2000) 157.
- [5] I.W.C.E. Arends, R.A. Sheldon, in: J.-E. Bäckvall (Ed.), *Modern Oxidation Methods*, Wiley-VCH, Weinheim, 2004, p. 83.
- [6] T. Mallat, A. Baiker, *Chem. Rev.* 104 (2004) 3037.
- [7] T. Matsumoto, M. Ueno, N. Wang, S. Kobayashi, *Chem. Asian J.* 3 (2008) 196.
- [8] K. Yamaguchi, N. Mizuno, *Angew. Chem., Int. Ed.* 41 (2002) 4538.
- [9] K. Yamaguchi, N. Mizuno, *Chem. Eur. J.* 9 (2003) 4353.
- [10] M. Matsumoto, N. Watanabe, *J. Org. Chem.* 49 (1984) 3435.
- [11] B.-Z. Zhan, M.A. White, T.-K. Sham, J.A. Pincock, R.J. Doucet, K.V.R. Rao, K.N. Robertson, T.S. Cameron, *J. Am. Chem. Soc.* 125 (2003) 2195.
- [12] D.V. Bavykin, A.A. Lapkin, P.K. Plucinski, J.M. Friedrich, *J. Catal.* 235 (2005) 10.
- [13] H. Yu, X. Fu, C. Zhou, F. Peng, H. Wang, J. Yang, *Chem. Commun.* (2009) 2408.
- [14] K. Yamaguchi, N. Mizuno, *Angew. Chem., Int. Ed.* 42 (2003) 1479.
- [15] J.W. Kim, K. Yamaguchi, N. Mizuno, *Angew. Chem., Int. Ed.* 47 (2008) 9246.
- [16] K. Yamaguchi, M. Matsushita, N. Mizuno, *Angew. Chem., Int. Ed.* 43 (2004) 1576.
- [17] K. Yamaguchi, T. Koike, M. Kotani, M. Matsushita, S. Shinachi, N. Mizuno, *Chem. Eur. J.* 11 (2005) 6574.
- [18] J.W. Kim, T. Koike, M. Kotani, K. Yamaguchi, N. Mizuno, *Chem. Eur. J.* 14 (2008) 4104.
- [19] H. Madhavaram, H. Idriss, S. Wendt, Y.D. Kim, M. Knapp, H. Over, J. Assmann, E. Löffler, M. Muhler, *J. Catal.* 202 (2001) 296.
- [20] Y.D. Kim, A.P. Seitsonen, S. Wendt, J. Wang, C. Fan, K. Jacobi, H. Over, G. Ertl, *J. Phys. Chem. B* 105 (2001) 3752.
- [21] K. Yamaguchi, T. Koike, J.W. Kim, Y. Ogasawara, N. Mizuno, *Chem. Eur. J.* 14 (2008) 11480.
- [22] D.A. McKeown, P.L. Hagans, L.P.L. Carette, A.E. Russell, K.E. Swider, D.R. Rolison, *J. Phys. Chem. B* 103 (1999) 4825.
- [23] M.J. Frisch, G.W. Trucks, H.B. Schlegel, G.E. Scuseria, M.A. Robb, J.R. Cheeseman, J.A. Montgomery Jr., T. Vreven, K.N. Kudin, J.C. Burant, J.M. Millam, S.S. Iyengar, J. Tomasi, V. Barone, B. Mennucci, M. Cossi, G. Scalmani, N. Rega, G.A. Petersson, H. Nakatsuji, M. Hada, M. Ehara, K. Toyota, R. Fukuda, J. Hasegawa, M. Ishida, T. Nakajima, Y. Honda, O. Kitao, H. Nakai, M. Klene, X. Li, J.E. Knox, H.P. Hratchian, J.B. Cross, V. Bakken, C. Adamo, J. Jaramillo, R. Gomperts, R.E. Stratmann, O. Yazyev, A.J. Austin, R. Cammi, C. Pomelli, J.W. Ochterski, P.Y. Ayala, K. Morokuma, G.A. Voth, P. Salvador, J.J. Dannenberg, V.G. Zakrzewski, S. Dapprich, A.D. Daniels, M.C. Strain, O. Farkas, D.K. Malick, A.D. Rabuck, K. Raghavachari, J.B. Foresman, J.V. Ortiz, Q. Cui, A.G. Baboul, S. Clifford, J. Cioslowski, B.B. Stefanov, G. Liu, A. Liashenko, P. Piskorz, I. Komaromi, R.L. Martin, D.J. Fox, T. Keith, M.A. Al-Laham, C.Y. Peng, A. Nanayakkara, M. Challacombe, P.M.W. Gill, B. Johnson, W. Chen, M.W. Wong, C. Gonzalez, J.A. Pople, *Gaussian 03, Revision D.02*, Gaussian Inc., Wallingford, CT, 2004.
- [24] D.D. Perrin, W.L.F. Armarego (Eds.), *Purification of Laboratory Chemicals*, third ed., Pergamon Press, Oxford, U.K., 1988, p. 80.
- [25] K. Yamaguchi, K. Mori, T. Mizugaki, K. Ebitani, K. Kaneda, *J. Am. Chem. Soc.* 122 (2000) 7144.
- [26] A. Dijkstra, A. Marino-González, A. Mairata i Payeras, I.W.C.E. Arends, R.A. Sheldon, *J. Am. Chem. Soc.* 123 (2001) 6826.
- [27] A. Hanyu, E. Takezaki, S. Sakaguchi, Y. Ishii, *Tetrahedron Lett.* 39 (1998) 5557.
- [28] I.V. Kozhevnikov, V.E. Tarabanko, K.I. Matveev, *Kinet. Catal.* 22 (1981) 619.
- [29] R.A. Sheldon, M. Wallau, I.W.C.E. Arends, U. Schuchardt, *Acc. Chem. Res.* 31 (1998) 485.
- [30] K.B. Sharpless, K. Akashi, K. Oshima, *Tetrahedron Lett.* 17 (1976) 2503.
- [31] S. Kanemoto, S. Matsubara, K. Takai, K. Oshima, K. Utimoto, H. Nozaki, *Bull. Chem. Soc. Jpn.* 61 (1988) 3607.
- [32] I.E. Markó, P.R. Giles, M. Tsukazaki, I. Chellé-Regnaud, C.J. Urch, S.M. Brown, *J. Am. Chem. Soc.* 119 (1997) 12661.
- [33] R. Lenz, S.V. Ley, *J. Chem. Soc., Perkin Trans. 1* (1997) 3291.
- [34] K.A. Connors, *Chemical Kinetics. The Study of Reaction Rates in Solution*, VCH Publishers Inc., New York, 1990. p. 293.